Stochastic Lotka-Volterra Dynamics in Macroeconomics: A Bounded Goodwin Wage-Employment Cycle

Areen Jain
Gretchen Whitney High School

Abstract

This paper analyzes wage–employment dynamics using a bounded stochastic Goodwin model formulated within a Lotka–Volterra framework. Employment and wage share are mapped into latent positive coordinates, preserving natural bounds while allowing nonlinear interactions and stochastic shocks. Simulation results based on Python implementations of stochastic differential equations validate the estimation framework, and the model is then estimated on U.S. quarterly data from 1960–2025 using an approximate maximum likelihood approach. Phase-space analysis reveals a persistent wage–employment loop, with employment leading wage share by approximately seven quarters. Stochastic simulations reproduce key features of observed persistence, highlighting the role of nonlinear feedback in macroeconomic labor dynamics.

Keywords: Goodwin cycle; wage share; employment dynamics; Lotka-Volterra systems; stochastic differential equations; nonlinear macroeconomics; phase-space analysis

1 Introduction

1.1 Background

This paper studies wage–employment dynamics using a bounded stochastic Goodwin model formulated within a Lotka–Volterra framework and implemented numerically in Python. Macroeconomic variables such as employment and income shares often exhibit persistent cyclical behavior that cannot be fully explained by exogenous shocks alone. An influential endogenous explanation is the Goodwin growth cycle, which models the interaction between employment and the wage share through distributive conflict: high employment strengthens workers' bargaining power and raises wages, while a higher wage share reduces profitability and dampens employment growth.[1]

The Goodwin model is mathematically analogous to the Lotka–Volterra predator–prey system, in which nonlinear interactions between populations produce cyclical dynamics. This analogy provides a useful framework for analyzing economic cycles using phase-space methods, equilibrium analysis, and invariant functions. However, direct application of the classical Lotka–Volterra model to economics is problematic because key variables such as employment rates and wage shares are naturally bounded between zero and one.[2] [3]

1.2 Literature Review

The first strand of the literature evaluates the Goodwin cycle using reduced-form econometric methods. Harvie (2000) provides the earliest systematic empirical test, examining ten OECD countries through log-linear regressions and ARDL-based Phillips curve specifications. Harvie finds that while estimated trajectories exhibit the characteristic anti-clockwise motion in the employment–wage share phase plane predicted by the Goodwin model, the implied equilibrium values deviate substantially from the data.[4] This result highlights the difficulty of reconciling the theoretical model with empirical magnitudes using simple regression techniques.

Subsequent studies apply similar reduced-form strategies to a wider set of economies. García Molina and Herrera Medina (2010) [5] extend Harvie's approach to both developed and developing countries, reporting persistent discrepancies between model-implied and observed wage share and employment dynamics. Moura and Ribeiro (2013) [6] examine the Brazilian economy using distributional methods and document qualitative anti-clockwise phase-plane movement, although quantitative deviations from the theoretical cycle remain significant.

A second strand of the literature seeks to improve empirical performance by modifying the Goodwin framework itself. Grasselli and Maheshwari (2018) [7] introduce capital accumulation into the wage-share equation, demonstrating that relatively small structural changes can substantially reduce estimation error while preserving cyclical behavior. Flaschel (2010) [8] emphasizes the importance of distinguishing between short-run and long-run Goodwin cycles in the U.S. economy, using HP-filtered data and two-stage least squares estimation to show that distributive cycles operate at different frequencies.

More recent contributions further generalize the Goodwin framework. Cauvel (2022) [9] decomposes the wage share into wages and productivity, allowing for richer interactions between utilization and distribution. Bailly, Mortier, and Giraud (2023) [10] extend the model to include financial variables, showing that Goodwin-type cycles persist when debt dynamics are incorporated.

A third strand of empirical work focuses on identifying growth regimes and temporal heterogeneity in wage–employment dynamics. Barrales and von Arnim (2017) [11] distinguish between short-run and long-run distributive cycles in the U.S. economy, finding evidence of regime switching between profit-led and wage-led dynamics. Barrales-Ruiz, von Arnim, and Rada (2021) [12] employ wavelet analysis and VAR impulse responses to further document frequency-dependent wage–employment interactions and regime shifts over time.

The present paper contributes to this literature by estimating the Goodwin mechanism directly as a bounded stochastic dynamical system. By formulating the model in latent continuous-time coordinates and mapping it into economically meaningful bounded variables, the approach preserves the nonlinear interaction at the core of the Goodwin cycle while allowing for stochastic shocks and formal likelihood-based inference. Empirical validation is conducted using phase-space diagnostics, deterministic skeleton analysis, and lead–lag structure, providing a complementary perspective to existing empirical approaches.

2 Data Description

2.1 Simulated Data

To establish internal validity and demonstrate parameter recovery in a controlled environment, the stochastic bounded Goodwin–Lotka–Volterra model is first analyzed using simulated data. Synthetic trajectories are generated from the proposed stochastic differential equations using prespecified parameter values treated as the data-generating process. This simulation-based approach allows isolation of the endogenous nonlinear dynamics implied by the model, abstracting from measurement error, structural breaks, and institutional features present in real macroeconomic data.

Latent state variables evolve in continuous time under multiplicative stochastic shocks and are mapped into economically meaningful bounded variables—the employment rate and wage share—using a monotone transformation that ensures values remain in the unit interval. Simulated trajectories are treated as observed data for likelihood-based estimation, providing a benchmark for assessing estimation accuracy prior to empirical application.

2.2 Empirical Data

To evaluate the empirical relevance of the bounded stochastic Goodwin model, the framework is subsequently applied to U.S. macroeconomic data. Quarterly observations spanning 1960Q1–2025Q3 are obtained from the Federal Reserve Economic Data (FRED) database.

Employment is proxied by the employment rate

$$E_t = 1 - \frac{\mathrm{UNRATE}_t}{100},$$

where UNRATE_t denotes the civilian unemployment rate (monthly). Monthly observations are aggregated to quarterly frequency by simple averaging. This measure yields a bounded employment rate in the unit interval and provides a standard indicator of labor market tightness.

The wage share is proxied by

$$W_t = \frac{\mathrm{COE}_t}{\mathrm{GDP}_t},$$

where COE_t denotes nominal compensation of employees and GDP_t denotes nominal gross domestic product, both observed at quarterly frequency. This ratio is widely used as an empirical measure of labor's share of income and exhibits slow-moving but persistent fluctuations over the sample period.

Both series are naturally bounded between zero and one and display low-frequency cyclical variation. To ensure consistency with the theoretical model, observed bounded variables (E_t, W_t) are mapped into latent positive coordinates via the inverse transformation

$$X_t = \frac{E_t}{1 - E_t}, \qquad Y_t = \frac{W_t}{1 - W_t}.$$

This transformation preserves ordering and monotonicity while allowing the latent state variables to evolve on the positive real line, as required by the stochastic Lotka–Volterra dynamics.

3 Model, Theory, and Estimation Framework

3.1 Deterministic Goodwin–Lotka–Volterra Model

We begin with a stylized Goodwin growth cycle describing the interaction between employment and the wage share. The model is formulated using a Lotka–Volterra–type structure, which captures nonlinear feedback between the two variables. In latent coordinates $X(t), Y(t) > 0$, the deterministic dynamics are given by

$$\dot{X}(t) = aX(t) - bX(t)Y(t),$$
$$\dot{Y}(t) = -cY(t) + dX(t)Y(t),$$

where $X(t)$ represents latent employment intensity and $Y(t)$ represents latent wage pressure. The parameters $a, b, c, d > 0$ govern baseline growth, interaction strength, and decay rates.

The system admits a coexistence equilibrium

$$(X^*, Y^*) = \left(\frac{c}{d}, \frac{a}{b}\right),$$

around which deterministic trajectories form closed orbits. These endogenous cycles arise from distributive conflict: high employment strengthens wage pressure, while rising wage pressure reduces employment growth.[13]

To ensure economically meaningful states, latent variables are mapped into bounded observed variables,

$$E(t) = \frac{X(t)}{1 + X(t)}, \qquad W(t) = \frac{Y(t)}{1 + Y(t)},$$

so that the employment rate $E(t)$ and wage share $W(t)$ lie in the unit interval.

3.2 Stochastic Extension

To account for aggregate economic uncertainty and unmodeled heterogeneity, the deterministic system is extended to a stochastic differential equation (SDE).[14] In latent coordinates, the model is given by

$$dX_t = \big(aX_t - bX_tY_t\big)\,dt + \sigma_X X_t\,dB_t^{(1)},$$
$$dY_t = \big(-cY_t + dX_tY_t\big)\,dt + \sigma_Y Y_t\,dB_t^{(2)},$$

where $B_t^{(1)}$ and $B_t^{(2)}$ are independent Brownian motions and $\sigma_X, \sigma_Y > 0$ control the intensity of stochastic shocks.

The use of multiplicative noise preserves positivity of the latent variables and implies that volatility scales with the level of economic activity. Observed variables E_t and W_t are obtained through the same bounded transformation as in the deterministic case. While stochastic shocks break exact conservation of deterministic invariants, the underlying cyclical structure persists, with randomness introducing irregular amplitude and phase variation.

3.3 Simulation of Trajectories

Model trajectories are generated numerically using standard discretization schemes. Deterministic paths are computed using Runge–Kutta methods, while stochastic trajectories are simulated using the Euler–Maruyama approximation.[15] For a fixed time step Δt, the latent stochastic dynamics are simulated recursively as

$$X_{t+\Delta t} = X_t + \mu_X(X_t, Y_t)\Delta t + \sigma_X X_t \sqrt{\Delta t}\, \varepsilon_t^{(1)},$$

with an analogous expression for Y_t, where $\varepsilon_t^{(i)} \sim \mathcal{N}(0,1)$.

Simulations are initialized away from equilibrium to reveal cyclical behavior. Both single trajectories and ensembles of trajectories are generated in order to study deterministic structure, stochastic diffusion, and variability across realizations.

3.4 Parameter Estimation

To demonstrate how model parameters can be estimated from data, we employ an approximate maximum likelihood approach based on the discretized stochastic system. Because closed-form transition densities for the nonlinear SDE are not available, the Euler–Maruyama approximation is used to derive tractable Gaussian conditional distributions.

Observed bounded variables (E_t, W_t) are first transformed back into latent coordinates via

$$X_t = \frac{E_t}{1 - E_t}, \qquad Y_t = \frac{W_t}{1 - W_t}.$$

Under the discretized model,

$$X_{t+1} \mid X_t, Y_t \sim \mathcal{N}\big(X_t + \mu_X(X_t, Y_t)\Delta t,\ (\sigma_X X_t)^2 \Delta t\big),$$

with a corresponding expression for Y_t. The log-likelihood is constructed by summing the Gaussian log-densities across time, and parameters $(a, b, c, d, \sigma_X, \sigma_Y)$ are estimated by numerical maximization. [16]

Estimation is illustrated using synthetic data generated from the model itself. This parameter recovery exercise allows us to assess identifiability and estimation accuracy in a controlled environment before considering empirical applications.

4 Results

We report results for the bounded stochastic Goodwin–Lotka–Volterra model using the baseline parameter vector $(a, b, c, d, \sigma_X, \sigma_Y) = (0.05, 0.08, 0.04, 0.06, 0.03, 0.03)$. The coexistence equilibrium in latent coordinates is $(X^*, Y^*) = (c/d,\ a/b) = (0.6667, 0.625)$, which maps to bounded economic variables $(E^*, W^*) = (X^*/(1+X^*),\ Y^*/(1+Y^*)) = (0.4000, 0.3846)$. All reported summary statistics are computed after discarding the first 20% of each trajectory as burn-in.

4.1 Stochastic Dynamics and Cycle Statistics

Introducing multiplicative stochastic shocks produces irregular yet persistent oscillations. For a representative stochastic trajectory (shown in Appendix Figure A1), post burn-in amplitudes are $A_E \approx 0.3102$ and $A_W \approx 0.3117$. Peak-based timing of employment cycles yields a mean period of $\bar{T} \approx 0.5364$ with standard deviation 0.1395 (358 detected peaks). To quantify variability under uncertainty, we simulate an ensemble of trajectories under the fitted model (Section 3.4). Across the ensemble, amplitude and period statistics are

$$A_E : 0.3089 \pm 0.1043, \qquad A_W : 0.2902 \pm 0.0989, \qquad \bar{T} : 0.5360 \pm 0.0076,$$

(mean $\pm$ standard deviation), showing that the stochastic system generates sustained cycles with substantial amplitude variability but relatively stable average timing.

4.2 Deterministic Dynamics

Under the deterministic system, trajectories remain bounded and exhibit cyclical variation around (E^*, W^*). For the baseline initialization used in this study, the post burn-in amplitudes are $A_E = \max(E) - \min(E) \approx 0.0711$ and $A_W \approx 0.0627$. The resulting orbit is small and close to equilibrium, and peak detection over the simulated horizon identifies only one post burn-in local maximum (hence a period estimate is not reported for this specific run). Phase-space plots and direction fields (see Appendix Figure A2) nonetheless show the characteristic closed-orbit structure of the Goodwin cycle. The invariant-function contours (Appendix Figure A3) further illustrate the nested cyclical structure around the equilibrium.

4.3 Parameter Estimation and Model Fit

Parameters were estimated from the simulated stochastic trajectory using approximate maximum likelihood based on Euler–Maruyama transition densities. The optimizer converged successfully, yielding

$$\hat{\theta} = (\hat{a}, \hat{b}, \hat{c}, \hat{d}, \hat{\sigma}_X, \hat{\sigma}_Y) = (0.0611, 0.0917, 0.0509, 0.0735, 0.02984, 0.03019).$$

Relative errors are small for diffusion parameters (below 1%) and moderate for drift parameters (approximately 15–27%), consistent with finite-sample identification challenges in nonlinear interaction models. Model fit was evaluated using an ensemble-based summary-statistic comparison: the observed cycle amplitudes lie near the center of the fitted ensemble distributions, with observed quantiles 0.527 for A_E and 0.580 for A_W and corresponding two-sided empirical p-values 0.947 and 0.840. Optional two-sample Kolmogorov–Smirnov tests on pooled marginal distributions reject equality at conventional levels, reflecting the sensitivity of KS tests under large pooled samples; accordingly, the main diagnostics emphasize cycle-relevant summary statistics (amplitude and period) and phase-space behavior.

5 Empirical Estimation and Results

5.1 Estimation Framework

The bounded stochastic Goodwin–Lotka–Volterra model is estimated on U.S. macroeconomic data using the same latent-state formulation as in the simulation analysis. Observed employment and wage share series are transformed into latent coordinates (X_t, Y_t) as described in Section 2.2. Parameters are estimated via approximate maximum likelihood using the Euler–Maruyama discretization with a quarterly time step. This ensures direct comparability between simulated and empirical results.

5.2 Parameter Estimates and Implied Equilibrium

The estimated drift coefficients imply an interior equilibrium

$$(X^*, Y^*) = \left(\frac{c}{d}, \frac{a}{b}\right), \qquad (E^*, W^*) = \left(\frac{X^*}{1+X^*}, \frac{Y^*}{1+Y^*}\right),$$

corresponding to $(E^*, W^*) \approx (0.947, 0.557)$. This equilibrium lies close to the empirical center of the observed employment and wage share series, indicating that the bounded nonlinear structure anchors the model to economically meaningful levels. Appendix Figure A4 compares the simulated trajectories from the fitted model against the observed data, demonstrating good alignment in both level and cyclical patterns.

5.3 Deterministic Cycles and Phase-Space Behavior

To isolate endogenous dynamics, the deterministic skeleton of the estimated model [Figure 1] is examined by setting diffusion terms to zero. Simulations of the deterministic system generate a closed phase-space orbit around the implied equilibrium, completing approximately two rotations over the sample horizon. This indicates the presence of a low-frequency endogenous cycle driven by nonlinear interaction between employment and wage pressure. Observed phase-space trajectories are irregular due to short-run shocks; however, smoothing the data reveals a persistent loop centered on the fitted equilibrium. Direction field analysis confirms that local drift forces induce rotation around the interior equilibrium rather than monotonic convergence.

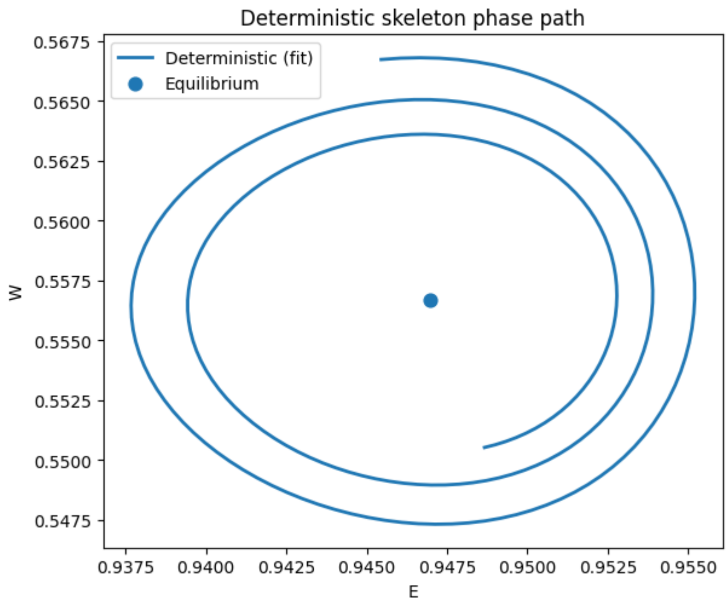

Figure 1: Smoothed Phase Plot with FRED Data

5.4 Rotation Direction and Lead–Lag Dynamics

The smoothed empirical phase trajectory exhibits a weak but systematic counterclockwise rotation, consistent with the qualitative predictions of the Goodwin model. Cross-correlation analysis shows that employment leads the wage share by approximately seven quarters, indicating a delayed wage response to labor market tightness. This lag structure aligns with the estimated interaction parameters, which imply slow wage adjustment relative to employment dynamics. [Figure 2] Together, the phase-space rotation and lead–lag evidence support a bargaining-power mechanism operating at low frequencies and partially obscured by short-run disturbances.

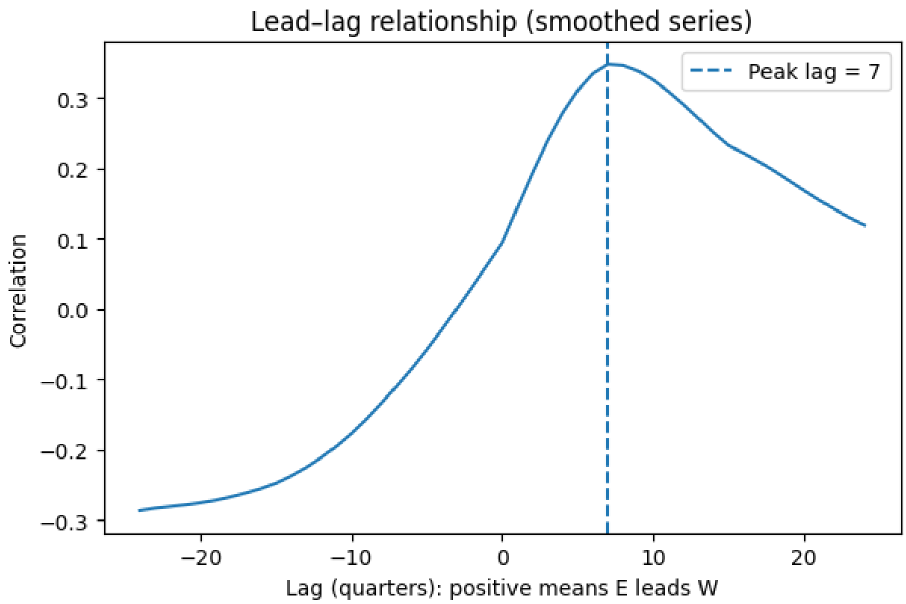

Figure 2: Lead-Lag Relationship between Employment and Wages

6 Discussion

6.1 Findings and Interpretation

The core finding is straightforward: high employment strengthens worker bargaining power, raising wages; elevated wages compress profit margins, eventually reducing employment; lower employment weakens wage pressure, restoring profitability and restarting the cycle. This represents a structural feature of market economies rather than a transitory disturbance.

This paper formalizes this mechanism using a bounded stochastic Lotka–Volterra framework. The empirical analysis confirms that the Goodwin cycle is an endogenous feature of the U.S. macroeconomy rather than an artifact of external shocks. The estimated equilibrium $(E^*, W^*) \approx (0.947, 0.557)$ serves as an attractor around which the economy rotates rather than a stable rest point. Stochastic shocks produce irregular yet persistent cycles: while peak timing exhibits relative stability (mean period $\bar{T} \approx 0.54$), cycle amplitudes vary substantially due to multiplicative noise.

For policy and forecasting, the implications are direct. Business cycles have an endogenous component that persists regardless of intervention. Attempting to permanently stabilize employment at high levels will generate wage pressure that inevitably reverses the expansion. Policymakers should design counter-cyclical tools that work with these oscillations rather than fighting them. Forecasters must treat employment and wages as a coupled system with stable average period but variable amplitude.

6.2 Future Research Directions

Several extensions would strengthen the empirical and theoretical foundations of this framework. First, incorporating capital accumulation dynamics would align the model more closely with Goodwin's original formulation and allow examination of investment–distribution interactions. Second, introducing heterogeneous agents or sectoral disaggregation could capture asymmetric responses across industries or income groups. Third, explicit modeling of monetary policy responses and inflation expectations would clarify the conditions under which policy can dampen or amplify endogenous cycles. Extending the analysis to a panel of countries or regions would test whether the estimated cycle parameters reflect universal structural features or country-specific institutions. While the current analysis establishes the presence and stability of endogenous cycles, normative evaluation requires explicit loss functions and constraints that balance stabilization objectives against distributional and efficiency considerations.

7 Supplemental Materials

The complete Python code, instructions on using the FRED dataset, and output graphs are available in the project's Github Repository for reproducibility and further exploration. The link is: https://github.com/areenjain09/StochasticLVDynamicsCycle

8 Acknowledgments

I am deeply grateful to Dr. Olga Korosteleva, Professor of Statistics at California State University, Long Beach, for her exceptional guidance and mentorship throughout this project. Her expertise and encouragement were pivotal in deepening my understanding of statistics and machine learning while nurturing my development as a researcher. I also wish to thank the teachers and mentors who have shaped my academic path and contributed to my growth. Finally, I extend profound thanks to my family for their unwavering love, steadfast encouragement, and constant presence throughout this journey. Their support has been indispensable.

A Appendix

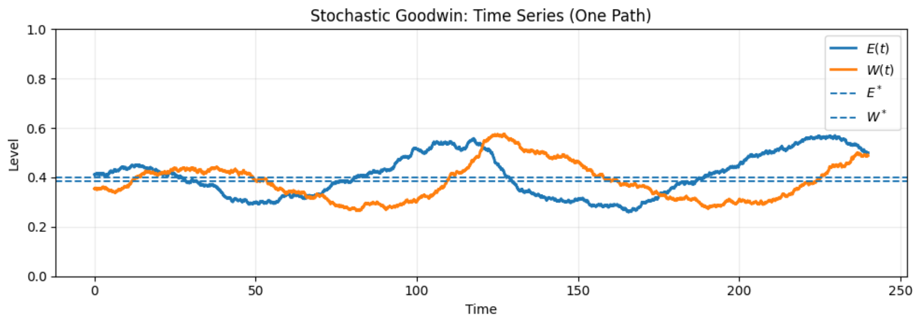

Figure A1: Simulated time series of employment and wage share under stochastic dynamics.

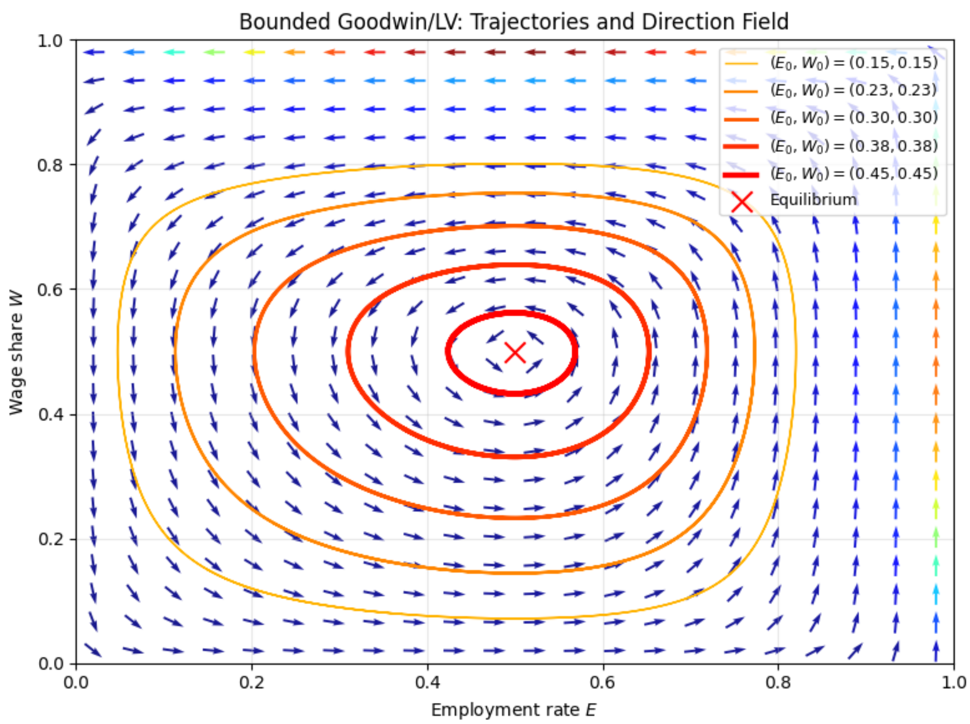

Figure A2: Phase-space direction field of the bounded Goodwin model.

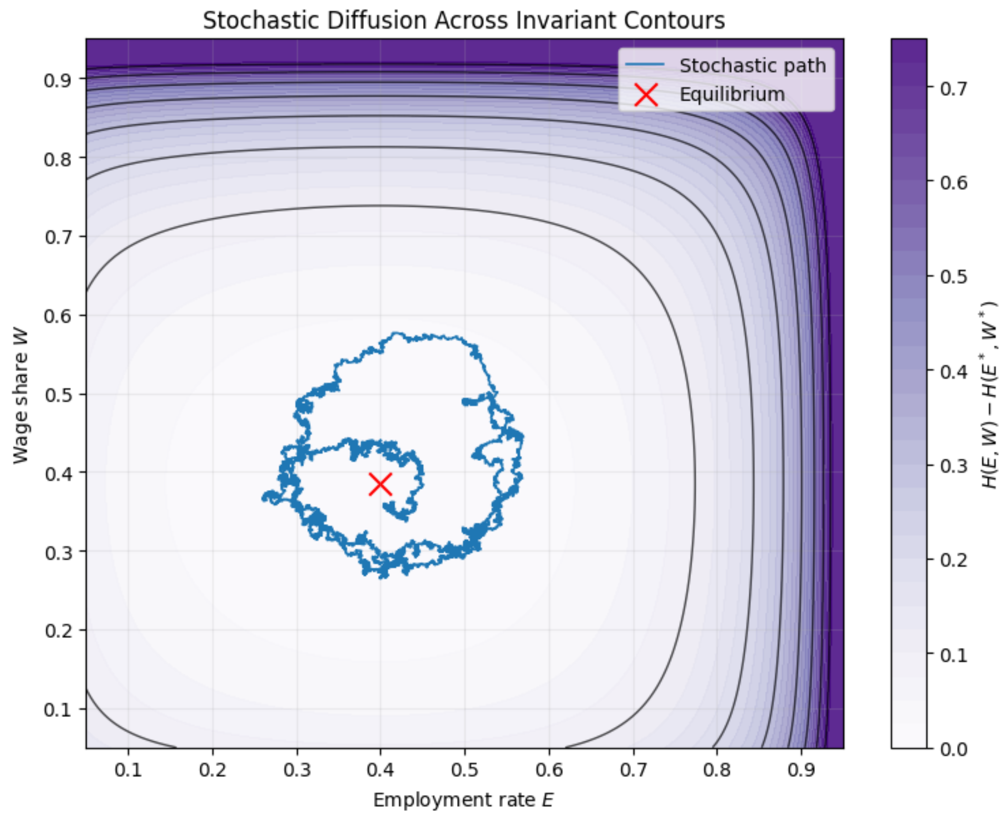

Figure A3: Invariant-function contours illustrating cyclical dynamics in phase space.

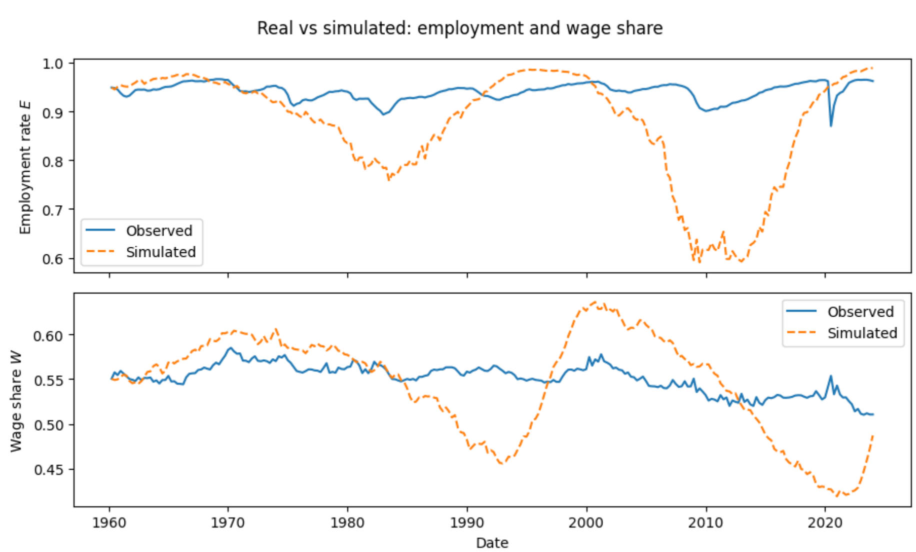

Figure A4: Real vs Simulated Data comparison of employment and wage share under stochastic dynamics.

References

[1] R. M. Goodwin, “A Growth Cycle,” in *Socialism, Capitalism and Economic Growth*, C. H. Feinstein, ed. Cambridge: Cambridge University Press, 1967, pp. 54–58.

[2] A. J. Lotka, *Elements of Physical Biology*. Baltimore: Williams & Wilkins, 1925.

[3] V. Volterra, “Fluctuations In The Abundance Of A Species Considered mathematically,” *Nature*, vol. 118, pp. 558–560, 1926.

[4] D. Harvie, *Testing Goodwin: Growth Cycles in Ten OECD Countries*, Cambridge Journal of Economics, vol. 24, no. 3, pp. 349–376, 2000.

[5] M. García Molina and E. Herrera Medina, *Empirical Evidence of Goodwin's Growth Cycle in Developed and Developing Countries*, International Journal of Social Economics, vol. 37, no. 5, pp. 365–383, 2010.

[6] R. L. Moura and R. S. M. Ribeiro, *An Empirical Analysis of the Goodwin Growth Cycle for Brazil*, Metroeconomica, vol. 64, no. 1, pp. 140–162, 2013.

[7] M. R. Grasselli and A. Maheshwari, *Testing a Goodwin Model with General Capital Accumulation Rate*, Metroeconomica, vol. 69, no. 3, pp. 619–643, 2018.

[8] P. Flaschel, *The Macrodynamics of Capitalism: Elements for a Synthesis of Marx, Keynes, and Schumpeter*, 2nd ed. Berlin: Springer, 2010.

[9] T. Cauvel, *Revisiting the Goodwin Growth Cycle: Productivity, Utilization, and Distribution*, Review of Political Economy, vol. 34, no. 4, pp. 610–633, 2022.

[10] A. Bailly, F. Mortier, and G. Giraud, *Empirical Analysis of a Debt-Augmented Goodwin Model for the United States*, Structural Change and Economic Dynamics, vol. 66, pp. 89–103, 2023.

[11] J. Barrales and R. von Arnim, *Distributional Cycles in the US Economy*, Cambridge Journal of Economics, vol. 41, no. 3, pp. 623–648, 2017.

[12] J. Barrales-Ruiz, R. von Arnim, and C. Rada, *Wage-Led versus Profit-Led Demand Regimes: A Wavelet Approach*, Structural Change and Economic Dynamics, vol. 58, pp. 289–305, 2021.

[13] S. H. Strogatz, *Nonlinear Dynamics and Chaos: With Applications to Physics, Biology, Chemistry, and Engineering*, 2nd ed. Boulder, CO: Westview Press, 2018.

[14] C. W. Gardiner, *Stochastic Methods: A Handbook for the Natural and Social Sciences*, 4th ed. Berlin: Springer, 2009.

[15] P. E. Kloeden and E. Platen, *Numerical Solution of Stochastic Differential Equations*. Berlin: Springer, 1992.

[16] S. M. Iacus, *Simulation and Inference for Stochastic Differential Equations: With R Examples*. New York: Springer, 2008.